Available online at www.sciencedirect.com
SCIENCE DIRECT®
PERGAMON
International Journal of Heat and Mass Transfer 46 (2003) 2065–2075
International Journal of HEAT and MASS TRANSFER
www.elsevier.com/locate/ijhmt

Determination of a heat source in porous medium with convective mass diffusion by an inverse method

M. Prud'homme *, S. Jasmin

Department of Mechanical Engineering, École Polytechnique de Montréal, C.P. 6079, Succ. Centre-ville, Montréal, Que., Canada H3C 3A7

Received 31 May 2002; received in revised form 11 October 2002

Abstract

A formulation is given of the inverse natural convection problem by conjugate gradient with adjoint equations in a porous medium with mass diffusion for the determination, from temperature measurements by sensors located within the medium, of an unknown volumetric heat source which is a function of the solute concentration. The direct, sensitivity and adjoint set of equations are derived for a Boussinesq fluid, over an arbitrary domain in two dimensions. Solutions by control volumes are presented for a square enclosure subjected to known temperature and concentration boundary conditions, assuming a source term depending on average vertical solute concentration. Reasonably accurate solutions are obtained at least up to $Ra = 10^5$ with the source models considered, for Lewis numbers ranging from 0.1 to 10. Noisy data solutions are regularized by stopping the iterations according to the discrepancy principle of Alifanov, before the high frequency components of the random noises are reproduced.

1. Introduction

It is generally acknowledged that the composting process of organic wastes helps to preserve environmental resources. Valuable constituents are also present in composting byproducts which can be successfully recovered for agricultural purposes. The experiments of Larsen and McCartney [1] with pulp and paper waste recently confirmed that composting is essentially a non-isothermal bioprocess, controlled by internal heat generation from microbial oxidation. They also reported strong relationships between microbial activity and chemical solute concentration ratios. Gostomski et al. [2] as well as Weppen [3] reached similar conclusions after their investigations and recognized the importance of humidity boundary conditions and how heat generation affects the microbiology.

In this context, it is relevant to seek efficient ways to determine either concentration and/or heat generation distribution within composting systems. From a modeling point of view, composting may be tough of as a double-diffusive convection problem in a porous medium with a heat source. Few studies were ever undertaken on this topic. Among these, Chamkha [4] recently treated the double-diffusive problem for a gas mixture contained in a rectangular enclosure with heat and mass gradients applied on the vertical walls and a heat source depending linearly upon temperature.

The inverse problem approach, which is purposely designed to estimate boundary conditions or thermophysical properties of a system where direct measurements are impracticable, offers an interesting way at this point to determine the heat source distributions within composting reactors. In most inverse heat transfer problems, one typically seeks to evaluate the temperature or heat flux on part of the boundary surface of a body, through the use of remote temperature measurements taken either within the body itself or on a different part of the bounding surface. Inverse problems are also characterized by the fact that small random errors

* Corresponding author. Tel.: +1-514-340-4711; fax: +1-514-340-5917.
E-mail address: miprud@meca.polymtl.ca (M. Prud'homme).

0017-9310/03/$ - see front matter © 2003 Elsevier Science Ltd. All rights reserved.
doi:10.1016/S0017-9310(02)00506-9

Nomenclature

A	area
$d\Omega$	boundary
E	error
f	arbitrary function
g	gravity
H	height
J	Jacobian
L	length
Le	Lewis number
n	normal direction
p	conjugate search direction
Q	volumetric heat Source
$\mathbf{r}$	position vector
Ra	Rayleigh number
S	solute concentration
t	time
T	temperature
$\mathbf{u}$	velocity vector
x, y	coordinates

Greek symbols

α	step size or thermal diffusivity
β	coefficient of thermal expansion
δ	Dirac delta function
Δ	increment
ε	small number or normalized porosity
σ	standard deviation
ψ	stream function
Ω	domain surface

Superscripts

k	iteration number
$\sim$	sensitivity variable
$-$	Adjoint variable
$\hat{}$	unit vector

Subscripts

av	average value
m	measurement value
0	reference value
f	final value
S	solute
T	thermal

Other symbols

$\langle \cdot \vert \cdot \rangle$	inner product
$\Vert \cdot \Vert$	norm
∇	gradient
$\nabla_n \times$	normal component of curls

in the internal measurements at the input can lead to substantial errors in the unknown boundary values at the output. Inverse problems are in mathematical terms classified as ill-posed problems, for which simple solution procedures such as the exact matching of the computational temperatures with the measurement values or a least squares minimization [5,6] of the error between calculations and measurements are prone to instability with inaccurate data.

A lot of efforts were consequently devoted over the last decades to the regularization of inverse solutions, that is, on how to reduce error growth. The function specification method of Beck and coworkers [7,8] where the time domain is subdivided and a least-squares problem solved over each subdomain in sequence, using assumptions about future data for stabilization, has emerged as what is probably the best known sequential procedure for inverse heat conduction problems.

Among the so-called whole domain methods, in which the unknown boundary condition or source term is determined at once for all times and/or positions, a solution procedure was developed by Tikhonov and Arsenin [9], which modifies the basic least squares method by adding a smoothing constraint term, multiplied by an appropriate regularization parameter. An alternative approach would be to rely on the iterative regularization method described by Alifanov [10]. Both methods are based on sound mathematical principles and are applicable to a large variety of inverse problems.

A lot of information is available in the literature regarding the inverse conduction problems encountered in the design, control and identification of thermal systems. Much less however can be found on inverse problems involving convection flow. This is especially true of problems in natural convection, for which the temperature and flow field equations are always non-linearly coupled. As a result, the problem is more difficult to solve than in forced convection. Let us mention that Moutsoglou [11] used the sequential function specification method to study laminar inverse natural convection in a vertical channel, for which the steady heat flux at one wall was the unknown, while the temperature on the opposite insulated wall was taken as known. More recently, Park and Chung [12] and later Park and Jung [13], solved the inverse natural convection problem for an unknown time-dependent heat source inside a square cavity, using the Chebyshev pseudospectral method and the Karhunen–Loève Galerkin method respectively, to solve the set of direct, adjoint and sensitivity equations. Zabaras and Yang [14] and Yang and Zabaras [15] used the conjugate gradient (CG) method to solve inverse natural convection problems by finite elements. Prud'homme and Nguyen [16] also choosed the CG method to solve the inverse natural convection problem,

in a square cavity with an unknown heat flux on one vertical wall, using adjoint equations.

In the present study, the CG method with adjoint equations will be adapted to solve the inverse natural convection problem in a porous medium with mass diffusion, for a volumetric heat source which is a function of the solute concentration, as could be found in a composting reactor for instance. The versatility of the method will be investigated by considering steady and unsteady problems, a linear and a non-linear source distribution model, in conduction and in convection.

The sensitivity and adjoint equations required by the CG method are derived in the following section over a simply connected domain in two dimensions, submitted to general linear boundary conditions. Numerical computations are carried out next for typical test cases in a simple rectangular geometry. Results are analyzed in terms of the Rayleigh and Lewis numbers to show the effects of diffusion on the stability and accuracy of the inverse solution. The influence of noisy input data on the solution will also be discussed.

2. Problem definition

The convective mass diffusion problem may be considered, at first, in the broad context of the arbitrary surface domain and boundary conditions summarized in Fig. 1. Let us assume from now on that the unknown heat source term Q is a function of the solute concentration S. Our goal is to derive the set of equations that will allow the determination of the source term Q over the time interval $0 \leqslant t \leqslant t_f$, from the temperature data T_m provided by the sensors. The boundary conditions on temperature and solute concentration are taken as known a priori, by specifying either the value of the function itself or its normal gradient on $d\Omega$. The initial temperature and concentration fields are also assumed to be known quantities when the convective process begins. The derivation of the inverse problem equations

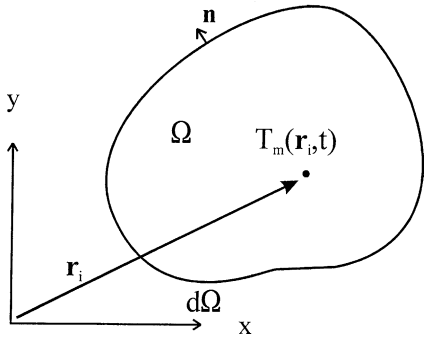

Fig. 1. Arbitrary solution domain.

is better carried out however in terms of dimensionless equations. An appropriate scaling of length, velocity, temperature, concentration and time is possible, based on

$$L, \quad \frac{\alpha}{L}, \quad \Delta T, \quad \Delta S, \quad \frac{\sigma L^2}{\alpha} \tag{1}$$

respectively, where all properties are taken as constants evaluated at some reference temperature T_0. The scales L, ΔT and ΔS may be left arbitrary at this point. The non-dimensional equations, in conservative form, governing temperature, stream function and concentration within the porous medium can then be expressed as

$$\begin{aligned} &\frac{\partial T}{\partial t} + \nabla \cdot (\mathbf{u}T - \nabla T) = Q \\ &\nabla^2 \psi = Ra \nabla_n \times (T\hat{\mathbf{g}}) \\ &\varepsilon \frac{\partial S}{\partial t} + \nabla \cdot \left(\mathbf{u}S - \frac{1}{Le} \nabla S \right) = 0 \end{aligned} \tag{2}$$

where Ra is the Rayleigh number and Le the Lewis number. The appropriate boundary conditions are the usual impermeability requirement on $d\Omega$, that is, $\psi = 0$ and

$$\begin{aligned} &T = f_T \quad \text{or} \quad \frac{\partial T}{\partial n} = g_T \\ &S = f_S \quad \text{or} \quad \frac{\partial S}{\partial n} = g_S \end{aligned} \tag{3}$$

for temperature and concentration, where the right-hand sides f_T, f_S and g_T, g_S may be functions of position and time. In general, both Dirichlet and Neumann conditions are admissible simultaneously for S and T, on different parts of the boundary $d\Omega$.

Solving the inverse problem for the unknown source term Q is an iterative process, based on a sequence of approximations $Q^0, Q^1, \ldots, Q^k$, and so on, based on some initial guess value Q^0, that will minimize the error

$$E(Q) = \frac{1}{2} \|T - T_m\|^2 \equiv \frac{1}{2} \int_0^{t_f} \sum_{i=1}^{n} (T - T_m)_i^2 \, dt \tag{4}$$

In the above, T and T_m stand respectively for the temperature predicted at the sensors from the source function approximation and the locally measured temperature. If Q is a function of time only, a single sensor, i.e. $n = 1$, is all that is really needed to obtain a valid solution. If Q is also a function of position of arbitrary form, however, a surface of sensors is needed in principle, which would require integration over Ω in Eq. (4). But since inverse equations are solved in discretized form, it is enough to assume a sensor at each computational point and to remain with the summation over the n locations in Eq. (4).

The sequence of approximations for the unknown heat source may be constructed following the steps of the well-known CG method [10,17], according to

$Q^{k+1} = Q^k + \alpha^k p^k$, where α^k is the step size and p^k the conjugate search direction. The search direction is related to the gradient of E with respect to Q, which can not be computed in the usual way without some prior assumptions about the shape of the function. In the general case, no such representation is available. The gradient of E and the step size α must be obtained respectively from the solution of the adjoint and sensitivity problems described below.

2.1. The sensitivity problem

Let us define the temperature sensitivity $\widetilde{T}$ as the directional derivative of T at Q in the direction ΔQ which is equal to

$$\widetilde{T} = \lim_{\varepsilon \to 0} \frac{T(Q + \varepsilon \Delta Q) - T(Q)}{\varepsilon} \tag{5}$$

and so on for the other two variables. Based on the definition of the sensitivity variables, it is straightforward to derive from Eq. (2) that the temperature, stream function and concentration sensitivities are solutions of the set of equations

$$\begin{aligned} &\frac{\partial \widetilde{T}}{\partial t} + \nabla \cdot (\mathbf{u}\widetilde{T} + \tilde{\mathbf{u}}T) - \nabla^2 \widetilde{T} = \Delta Q \\ &\nabla^2 \widetilde{\psi} = Ra \nabla_{\mathrm{n}} \times (\widetilde{T}\hat{\mathbf{g}}) \\ &\varepsilon \frac{\partial \widetilde{S}}{\partial t} + \nabla \cdot (\mathbf{u}\widetilde{S} + \tilde{\mathbf{u}}S) - \frac{1}{Le}\nabla^2 \widetilde{S} = 0 \end{aligned} \tag{6}$$

It is further shown that the sensitivity variables must satisfy the homogeneous counterparts of the direct variables initial and boundary conditions. Thus, the appropriate condition for the stream function sensitivity is $\widetilde{\psi} = 0$, while for the other sensitivity variables, the requirements are

$$\begin{aligned} &\widetilde{T} = 0 \quad \text{or} \quad \frac{\partial \widetilde{T}}{\partial n} = 0 \\ &\widetilde{S} = 0 \quad \text{or} \quad \frac{\partial \widetilde{S}}{\partial n} = 0 \end{aligned} \tag{7}$$

2.2. The adjoint problem

The directional derivative of E can be used to define the gradient ∇E of E with respect to Q from the formal equality

$$D_{\Delta Q}E(Q) = \langle \nabla E | \Delta Q \rangle \tag{8}$$

where the inner product on the right-hand side is to be understood in a general way. The gradient of E can be determined as part of the solution of a set of adjoint equations as follows. Starting from Eq. (4), the directional derivative of E is

$$D_{\Delta Q}E(Q) = \langle T - T_{\mathrm{m}} | \widetilde{T} \rangle \equiv \int_0^{t_{\mathrm{f}}} \sum_{i=1}^{n} (T - T_{\mathrm{m}})_i \widetilde{T}_i \, \mathrm{d}t \tag{9}$$

where all quantities are evaluated at the sensors positions. It can be noticed that the expression on the right-hand side of Eq. (9) may be expressed using Dirac's delta function as an integral over surface and time. Introducing the so-called adjoint temperature $\overline{T}$, concentration $\overline{S}$, stream function $\bar{\psi}$, it is possible to substitute Eq. (6) into Eq. (9) to get

$$\begin{aligned} D_{\Delta Q}E(Q) = &\int_0^{t_{\mathrm{f}}} \int_\Omega (T - T_{\mathrm{m}}) \widetilde{T} \sum_{i=1}^{n} \delta(\mathbf{r} - \mathbf{r}_i) \, \mathrm{d}A \, \mathrm{d}t \\ &+ \int_0^{t_{\mathrm{f}}} \int_\Omega \bar{\psi} \{ \nabla^2 \widetilde{\psi} - Ra \nabla_{\mathrm{n}} \times (\widetilde{T}\hat{\mathbf{g}}) \} \, \mathrm{d}A \, \mathrm{d}t \\ &+ \int_0^{t_{\mathrm{f}}} \int_\Omega \overline{T} \Bigg\{ \frac{\partial \widetilde{T}}{\partial t} + \nabla \cdot (\mathbf{u}\widetilde{T} + \tilde{\mathbf{u}}T) \\ &\quad - \nabla^2 \widetilde{T} - \Delta Q \Bigg\} \mathrm{d}A \, \mathrm{d}t \\ &+ \int_0^{t_{\mathrm{f}}} \int_\Omega \overline{S} \Bigg\{ \varepsilon \frac{\partial \widetilde{S}}{\partial t} + \nabla \cdot (\mathbf{u}\widetilde{S} + \tilde{\mathbf{u}}S) \\ &\quad - \frac{1}{Le} \nabla^2 \widetilde{S} \Bigg\} \mathrm{d}A \, \mathrm{d}t \end{aligned} \tag{10}$$

By virtue of the Green's identities, the divergence theorem, and the impermeability condition on the boundary $\mathrm{d}\Omega$, it follows from Eq. (10) that

$$\begin{aligned} D_{\Delta Q}E(Q) = &\int_0^{t_{\mathrm{f}}} \int_\Omega (T - T_{\mathrm{m}}) \widetilde{T} \sum_{i=1}^{n} \delta(\mathbf{r} - \mathbf{r}_i) \, \mathrm{d}A \, \mathrm{d}t \\ &+ \int_0^{t_{\mathrm{f}}} \int_\Omega \{ \widetilde{\psi} \nabla^2 \bar{\psi} - Ra \bar{\psi} \nabla_{\mathrm{n}} \times (\widetilde{T}\hat{\mathbf{g}}) \} \, \mathrm{d}A \, \mathrm{d}t \\ &+ \int_0^{t_{\mathrm{f}}} \int_\Omega \Bigg\{ \overline{T} \frac{\partial \widetilde{T}}{\partial t} - \widetilde{T}(\mathbf{u} \cdot \nabla)\overline{T} - T(\tilde{\mathbf{u}} \cdot \nabla)\overline{T} \\ &\quad - \widetilde{T} \nabla^2 \overline{T} - \overline{T} \Delta Q \Bigg\} \mathrm{d}A \, \mathrm{d}t \\ &+ \int_0^{t_{\mathrm{f}}} \int_\Omega \Bigg\{ \varepsilon \overline{S} \frac{\partial \widetilde{S}}{\partial t} - \widetilde{S}(\mathbf{u} \cdot \nabla)\overline{S} - S(\tilde{\mathbf{u}} \cdot \nabla)\overline{S} \\ &\quad - \frac{\widetilde{S}}{Le} \nabla^2 \overline{S} \Bigg\} \mathrm{d}A \, \mathrm{d}t \\ &+ \int_0^{t_{\mathrm{f}}} \oint_{\mathrm{d}\Omega} \Bigg(\bar{\psi} \frac{\partial \widetilde{\psi}}{\partial n} - \widetilde{\psi} \frac{\partial \bar{\psi}}{\partial n} + \widetilde{T} \frac{\partial \overline{T}}{\partial n} - \overline{T} \frac{\partial \widetilde{T}}{\partial n} \\ &\quad + \frac{\widetilde{S}}{Le} \frac{\partial \overline{S}}{\partial n} - \frac{\overline{S}}{Le} \frac{\partial \widetilde{S}}{\partial n} \Bigg) \mathrm{d}l \, \mathrm{d}t \end{aligned} \tag{11}$$

Each term in the boundary integral on the right-hand side of Eq. (11) does vanish on some part of $\mathrm{d}\Omega$, as a consequence of the boundary conditions imposed upon the sensitivity variables. If the adjoint variables are re-

quired to satisfy the same boundary conditions, that is, $\bar{\psi} = 0$ for the adjoint stream function and

$$\begin{aligned} &\overline{T} = 0 \quad \text{or} \quad \frac{\partial \overline{T}}{\partial n} = 0 \\ &\overline{S} = 0 \quad \text{or} \quad \frac{\partial \overline{S}}{\partial n} = 0 \end{aligned} \tag{12}$$

for the adjoint temperature and concentration, respectively, the boundary integral disappears from Eq. (11). The directional derivative can then be expressed using continuity as

$$\begin{aligned} D_{\Delta Q}E(Q) = &\int_0^{t_f}\int_\Omega (T - T_m)\widetilde{T}\sum_{i=1}^{n}\delta(\mathbf{r}-\mathbf{r}_i)\,\mathrm{d}A\,\mathrm{d}t \\ &+ \int_0^{t_f}\int_\Omega \{\widetilde{\psi}\nabla^2\bar{\psi} - Ra\bar{\psi}\nabla_n\times(\widetilde{T}\hat{\mathbf{g}})\}\,\mathrm{d}A\,\mathrm{d}t \\ &+ \int_0^{t_f}\int_\Omega \left\{\overline{T}\frac{\partial\widetilde{T}}{\partial t} - \widetilde{T}\nabla\cdot\left(\mathbf{u}\overline{T} + \nabla\overline{T}\right)\right. \\ &\left. - T(\tilde{\mathbf{u}}\cdot\nabla)\overline{T} - \overline{T}\Delta Q\right\}\mathrm{d}A\,\mathrm{d}t \\ &+ \int_0^{t_f}\int_\Omega \left\{\varepsilon\overline{S}\frac{\partial\widetilde{S}}{\partial t} - \widetilde{S}\nabla\cdot\left(\mathbf{u}\overline{S} + \frac{1}{Le}\nabla\overline{S}\right)\right. \\ &\left. - S(\tilde{\mathbf{u}}\cdot\nabla)\overline{S}\right\}\mathrm{d}A\,\mathrm{d}t \end{aligned} \tag{13}$$

after a slight rearrangement of terms. The following identities hold as a consequence of the stream function properties

$$\begin{aligned} T(\tilde{u}\cdot\nabla)\overline{T} &= -\nabla_n\times(T\widetilde{\psi}\nabla\overline{T}) + \widetilde{\psi}J(T,\overline{T}) \\ S(\tilde{u}\cdot\nabla)\overline{S} &= -\nabla_n\times(S\widetilde{\psi}\nabla\overline{S}) + \widetilde{\psi}J(S,\overline{S}) \end{aligned} \tag{14}$$

and can be verified by expanding both sides. It is straightforward to show also that

$$\bar{\psi}\nabla_n\times(\widetilde{T}\hat{\mathbf{g}}) = \nabla_n\times(\bar{\psi}\widetilde{T}\hat{\mathbf{g}}) - \widetilde{T}\nabla_n\times(\bar{\psi}\hat{\mathbf{g}}) \tag{15}$$

since gravity is a constant vector.

It follows from Eqs. (13)–(15) and the boundary conditions on the sensitivity and adjoint stream function that

$$\begin{aligned} D_{\Delta Q}E(Q) = &\int_0^{t_f}\int_\Omega (T - T_m)\widetilde{T}\sum_{i=1}^{n}\delta(\mathbf{r}-\mathbf{r}_i)\,\mathrm{d}A\,\mathrm{d}t \\ &+ \int_0^{t_f}\int_\Omega \widetilde{\psi}\{\nabla^2\bar{\psi} - J(T,\overline{T}) - J(S,\overline{S})\}\,\mathrm{d}A\,\mathrm{d}t \\ &+ \int_0^{t_f}\int_\Omega \left\{\overline{T}\frac{\partial\widetilde{T}}{\partial t} - \widetilde{T}\nabla\cdot(\mathbf{u}\overline{T} + \nabla\overline{T})\right. \\ &\left. + Ra\widetilde{T}\nabla_n\times(\bar{\psi}\hat{\mathbf{g}}) - \overline{T}\Delta Q\right\}\mathrm{d}A\,\mathrm{d}t \\ &+ \int_0^{t_f}\int_\Omega \left\{\varepsilon\overline{S}\frac{\partial\widetilde{S}}{\partial t} - \widetilde{S}\nabla\cdot\left(\mathbf{u}\overline{S} + \frac{1}{Le}\nabla\overline{S}\right)\right\}\mathrm{d}A\,\mathrm{d}t \end{aligned} \tag{16}$$

after using Green's theorem. The next step is to assume that the adjoint temperature and concentration both vanish at $t = t_f$, so that Eq. (16) can be simplified further as

$$\begin{aligned} D_{\Delta Q}E(Q) = &\int_0^{t_f}\int_\Omega -\overline{T}\Delta Q\,\mathrm{d}A\,\mathrm{d}t \\ &+ \int_0^{t_f}\int_\Omega \widetilde{\psi}\{\nabla^2\bar{\psi} - J(T,\overline{T}) - J(S,\overline{S})\}\,\mathrm{d}A\,\mathrm{d}t \\ &+ \int_0^{t_f}\int_\Omega \widetilde{T}\left\{-\frac{\partial\overline{T}}{\partial t} - \nabla\cdot(\mathbf{u}\overline{T} + \nabla\overline{T})\right. \\ &\left. + Ra\nabla_n(\bar{\psi}\hat{\mathbf{g}}) + (T - T_m)\sum_{i=1}^{n}\delta(\mathbf{r}-\mathbf{r}_i)\right\}\mathrm{d}A\,\mathrm{d}t \\ &- \int_0^{t_f}\int_\Omega \widetilde{S}\left\{\varepsilon\frac{\partial\overline{S}}{\partial t} + \nabla\cdot\left(\mathbf{u}\overline{S} + \frac{1}{Le}\nabla\overline{S}\right)\right\}\mathrm{d}A\,\mathrm{d}t \end{aligned} \tag{17}$$

by interchanging the order of integration for the time derivatives and using the initial conditions for the sensitivity variables. All the terms between brackets in Eq. (17) above vanish if

$$\begin{aligned} &\nabla^2\bar{\psi} = J(T,\overline{T}) + J(S,\overline{S}) \\ &\frac{\partial\overline{T}}{\partial t} + \nabla\cdot(\mathbf{u}\overline{T} + \nabla\overline{T}) = (T - T_m)\sum_{i=1}^{n}\delta(\mathbf{r}-\mathbf{r}_i) \\ &\qquad\qquad + Ra\nabla_n\times(\bar{\psi}\hat{\mathbf{g}}) \\ &\varepsilon\frac{\partial\overline{S}}{\partial t} + \widetilde{S}\nabla\cdot\left(\mathbf{u}\overline{S} + \frac{1}{Le}\nabla\overline{S}\right) = 0 \end{aligned} \tag{18}$$

The set of equations in Eq. (18) defines the adjoint problem, together with the homogeneous conditions imposed on the adjoint variables on the boundary $\mathrm{d}\Omega$ and at time $t = t_f$. It should be mentioned at this point that the change of variable $\tau = t_f - t$ has to be made first, in order to solve the adjoint equation with the "end condition" at the physical time $t = t_f$. Via this transformation, the adjoint problem becomes an initial value problem in τ.

Finally, only one term remains on the right-hand side of Eq. (17)

$$D_{\Delta Q}E(Q) = \int_0^{t_f}\int_\Omega -\overline{T}\Delta Q\,\mathrm{d}A\,\mathrm{d}t \equiv \langle -\overline{T}|\Delta Q\rangle \tag{19}$$

The conclusion from Eqs. (8) and (19) is, that the gradient of the error functional for an arbitrary source $Q(\mathbf{r},t)$ is equal to minus the local adjoint temperature, in other words, $\nabla E = -\overline{T}$. This result is valid irrespective of the actual shape of the solution domain or of the specific form of the boundary conditions imposed on the variables. Nevertheless, the computational tests are performed here in a simple square cavity geometry, under the boundary conditions summarized in Fig. 2 for

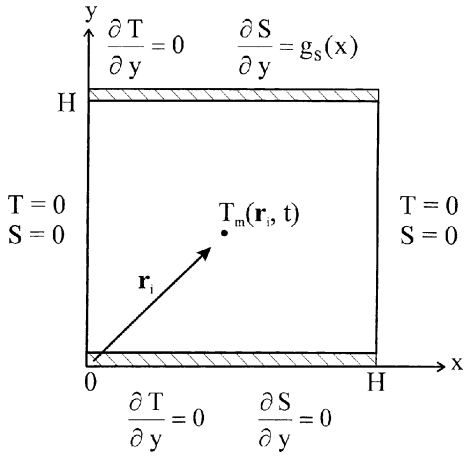

Fig. 2. Test computation geometry and coordinate system.

S and T. The scalings in Eq. (1) are then done with respect to the width of the cavity. Simple models are considered from now on for the heat source. At first, a linear model assuming that Q is equal to the average solute concentration in the vertical direction

$$Q(x,t) = S_{\mathrm{av}}(x,t) \equiv \int_0^1 S(x,y,t)\,\mathrm{d}y \tag{20}$$

Secondly, a non-linear model based on the average solute concentration in the vertical direction, namely

$$Q(x,t) = \mathrm{erf}[100 S_{\mathrm{av}}(x,t)] \tag{21}$$

where the multiplicative factor 100 was selected by experimentation so as to ensure significant levels of non-linearity of the source term Q. For both models, a slight modification is required to the definition of the gradient of the error functional, which is then equal to equal to minus the average over y of the adjoint temperature

$$\nabla E(x,t) = -\overline{T}_{\mathrm{av}}(x,t) \tag{22}$$

3. Method of conjugate gradient

The overall CG algorithm may be summarized as follows [10,17]:

1. Set initial conditions and choose initial guess Q^0. Set iteration counter $k = 0$.
2. Solve the direct problem with Q^k to obtain T^k.
3. Evaluate the error $T^k - T_{\mathrm{m}}$ at the sensors positions.
4. Solve the adjoint problem backward in time to obtain $\overline{T}^k$.
5. Evaluate the gradient ∇E^k from $\overline{T}^k$ according to Eq. (22).
6. Calculate the search direction p^k. If $k = 0$, $p^k = -\nabla E^k$, otherwise, $p^k = -\nabla E^k + \gamma^k p^{k-1}$ with

$$\gamma^k = \frac{\langle \nabla E^k - \nabla E^{k-1} | \nabla E^k \rangle}{\| \nabla E^{k-1} \|^2}$$

7. Solve the sensitivity problem with $\Delta Q = p^k$ on domain Ω to obtain $\widetilde{T}^k$ at the sensors positions.
8. Calculate the step size

$$\alpha^k = -\frac{\langle T^k - T_{\mathrm{m}} | \widetilde{T}^k \rangle}{\| \widetilde{T}^k \|^2}$$

9. Update to $Q^{k+1} = Q^k + \alpha^k p^k$.
10. Set $k \leftarrow k + 1$, go back to step 2, repeat until convergence criterion $E^k < \varepsilon E^0$ is satisfied.

In the above, the errors $E^0, E^1, \ldots, E^n$ are evaluated from the current estimates $T^0, T^1, \ldots, T^n$ of the temperature field computed using the estimates $Q^0, Q^1, \ldots$ and so on. The discrepancy principle [12] can be used to select a value for the small number ε in the convergence criterion when the temperature data contain random errors with uniform distribution. The criterion expression $\varepsilon = \sigma^2$ is easily derived using Eq. (4) from the assumption that $T^n - T_{\mathrm{m}} \approx \sigma T_{\mathrm{m}}$ where σ is the standard deviation of the measurements, which is taken as a known constant. Nevertheless, this criterion remains only a guideline and it is advisable to check the inverse solution obtained at iteration steps prior to the satisfaction of the criterion when the data contain noise. It can also happen that the error levels out at a value slightly above σ^2 after a few iterations. In the case of exact data however, the stopping criterion was set at $\varepsilon = 2.5 \times 10^{-5}$ for all the results presented in the next section.

4. Results and discussion

The direct, sensitivity and adjoint problems described earlier are solved by finite-differences using the control volume method and a first-order implicit time scheme. All the computations are performed for a 41 by 41 uniform mesh, with a time step $\Delta t = \Delta\tau$ ranging from 5×10^{-3} to 1.5×10^{-2} depending on the value of the Lewis number. A row of sensors, with one sensor at every computational point along x, is located at $y = 0.5$ unless mentioned otherwise. The initial conditions used are always $T = S = \psi = 0$ and the simulation time t_{f} is selected so that a steady-state solution is reached in every case considered.

Let us recall that the inverse solution for the source term at t_{f} is always equal to the initial guess value, since the adjoint temperature field is always equal to zero at the final time t_{f}. Even though the CG method can be modified to alleviate this difficulty [12], it is possible to take advantage of the existence of a steady-state solution by using only the adjoint temperature at the final τ value

in the conjugate direction. In this case, the computations can start from $Q^0 = 0$ as initial guess for the source term. Alternatively, if one is interested in the transient regime, the steady-state source distribution can be used as the initial guess value, once it has been determined. The discussion will now focus on the effects of Rayleigh and Lewis numbers, and random errors on the inverse solutions obtained by the present method for the test geometry sketched in Fig. 2.

4.1. Molecular diffusion regime

When the Rayleigh number Ra is equal to zero, the direct as well as the inverse problems are linear and superposition of solutions becomes possible. Without loss of generality, it is enough then to examine the efficiency of the inverse solution procedure for a concentration flux made up of a single space Fourier component on the top boundary of the domain in Fig. 2. For a flux $g_S(x) = \sin(n\pi x)$ at $y = 1$ therefore, the steady mass diffusion equation in Eq. (2) reduces to the Laplace equation $\nabla^2 S = 0$ when $Ra = 0$. This equation admits for the boundary conditions summarized in Fig. 2 the exact solution

$$S(x,y) = \frac{\cosh(n\pi y)}{n\pi \sinh(n\pi)} \sin(n\pi x) \tag{23}$$

According to our linear test model for the relationship between solute concentration and volumetric heat generation, the heat source distribution term is in this case

$$Q(x) = \frac{\sin(n\pi x)}{n^2\pi^2} \tag{24}$$

Considering the thermal boundary conditions given in Fig. 2, the temperature field must be independent of y and the steady-state solution for T is simply proportional to the source term

$$T(x) = \frac{\sin(n\pi x)}{n^4\pi^4} \tag{25}$$

Let us first consider the steady inverse solution obtained for a concentration flux $g_S(x) = \sin(\pi x)$ imposed at $y = 1$. Since the temperature field is independent of y, the vertical positioning of the sensors is irrelevant. The inverse solution is independent of the height of the sensors in the enclosure in this case and also of the porosity and the Lewis number. The heat source profile obtained from the direct problem solution with the concentration flux g_S is shown at $t = t_f$ in Fig. 3 along with the analytical solution given by Eq. (24) for $n = 1$. The slight discrepancy between the numerical and analytical solutions is due to the discretization error and can be reduced by refining the grid. Also shown on Fig. 3 is

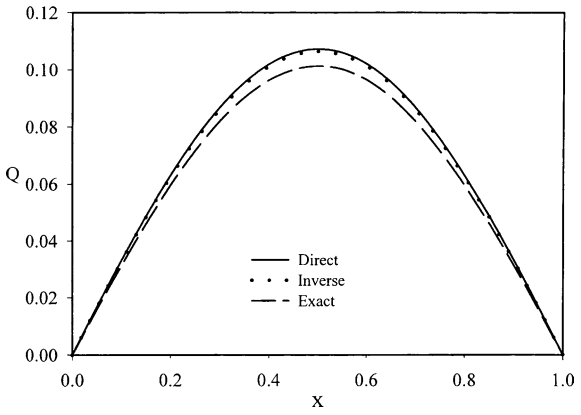

Fig. 3. Predicted heat source profiles at t_f, $g_S(x) = \sin(\pi x)$, $Ra = 0$.

the heat source profile predicted from the steady inverse solution, starting from the estimate $Q^0 = 0$. It is clear therefore that the inverse solution procedure can predict with success an unknown heat source of the form $Q = \sin(\pi x)$. Since the inverse problem is linear when $Ra = 0$ and steady, convergence is achieved after a single iteration, as expected under these circumstances.

The effect of noisy input data on the inverse solution is examined next. The transient inverse solution for $Ra = 0$ obtained for a noise of relative standard deviation $\sigma = 0.04$ is shown in Fig. 4. The evolution of the error, normalized by E^0, with the number of iterations is also plotted. The reasonably accurate solution obtained after 3 iterations, starting from the steady solution of the direct problem as initial guess for Q^0, appears far more satisfactory than the solution obtained after 11 iterations. The difference between the solutions is a clear indication of the iterative regularization effect of the CG

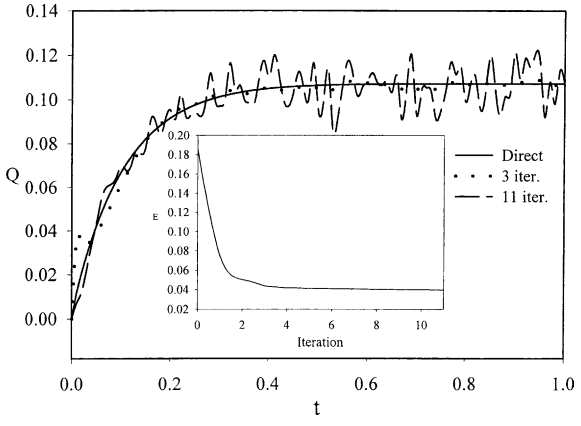

Fig. 4. Heat source prediction versus time at $x = 0.5$, noisy data, $g_S(x) = \sin(\pi x)$, $Le = 1$, $Ra = 0$, $\sigma = 0.04$.

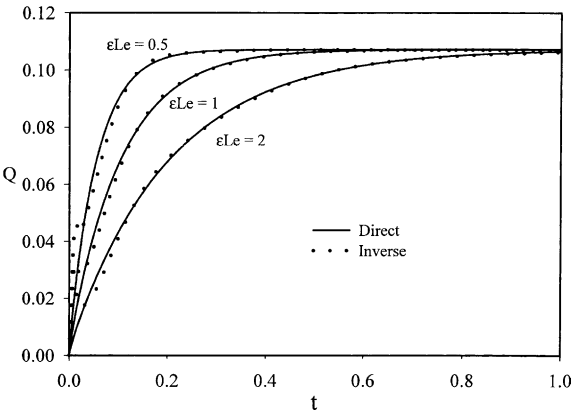

Fig. 5. Heat source prediction versus time at $x = 0.5$. Influence of εLe, $g_S(x) = \sin(\pi x)$, $Ra = 0$.

method. This phenomenon can be used with profit to optimise the final result. It has been observed on many occasions, as by Prud'homme and Nguyen [18] in inverse conduction for instance, that the multiple frequency components of an inverse solution are not reproduced at the same rate by the algorithm, but rather successively from the lower to the higher frequencies. This sequential convergence is at the origin of the regularisation effect. Optimisation of the solution is therefore feasible by merely stopping the iterations before the high frequency solution components, essentially due to the noise, are recovered.

Fig. 5 shows the transient direct and inverse solutions for different values of the product εLe, which controls the time needed for the solutions to reach the common steady-state value. Convergence is achieved in 8 iterations for $\varepsilon Le = 0.5$ and 1 and only 6 iterations for $\varepsilon Le = 2$. Nevertheless, the overall level of agreement between the direct and inverse solutions is quite good in all the cases considered.

4.2. Convection regime

By setting the Rayleigh number Ra equal to 10^5, the influence of convective flow within the cavity becomes significant, as can be seen in Fig. 6, which shows the direct solution isotherms, streamlines and isoconcentration lines obtained at $t = t_f$ for $g_S = \sin(\pi x)$ and $Le = 1$. It is obvious from the isotherm pattern that there is a definite temperature stratification over most of the cavity at this Rayleigh number. Consequently, the sensors position along y is expected to matter in this case in the accuracy of the inverse solution. The streamlines shown on Fig. 6 correspond to a pair of counter-rotating convection cells which are also found for other Rayleigh and Lewis numbers but with different intensities. There is also a significant stratification of concentration near the top of the cavity, indicating that a concentration boundary layer is forming along the wall.

Fig. 7 describes the influence of the Lewis number on the distribution of the solute concentration within the cavity. It is seen from Figs. 6 and 7 that, even at a fairly high Ra value, the Lewis number strongly affects both the magnitude and spatial distribution of the solute concentration S. As Le increases, the level of solute concentration becomes weaker over the bulk of the cavity. Consequently, the heat source Q also becomes weaker for the present model. The distribution of S also evolves from a rather smooth stratification for $Le = 0.1$ to a definite boundary layer for $Le = 10$. On the other hand, the shape of the isotherms and streamlines is not affected much by the Lewis number.

Satisfactory inverse solutions can be obtained at $Ra = 10^5$ as shown in Fig. 8. The steady heat source profiles are displayed versus x for different values of Le. It is noticed that the source becomes weaker as Le increases, as expected, because the solute concentration becomes weaker too. More iterations are required to achieve convergence and the source profile is also not

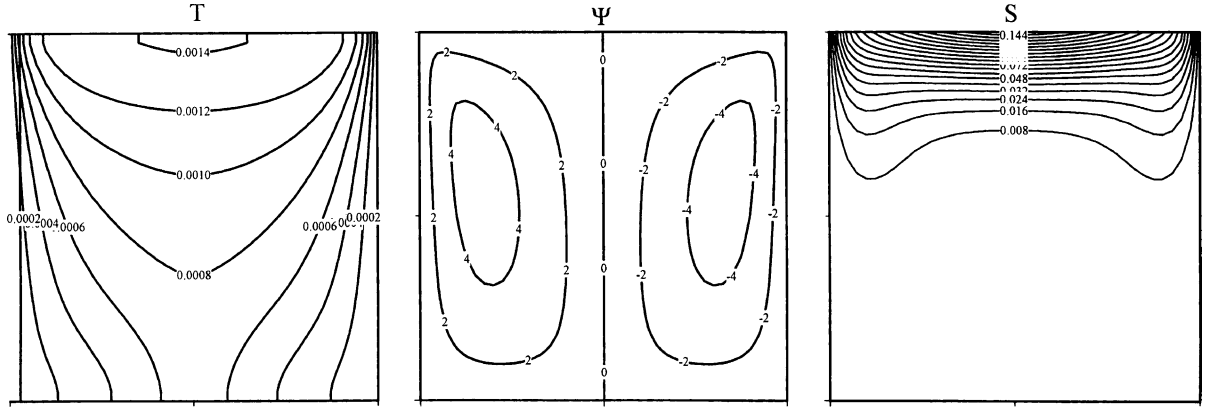

Fig. 6. Steady isocontours, $g_S(x) = \sin(\pi x)$, $Le = 1$, $Ra = 10^5$.

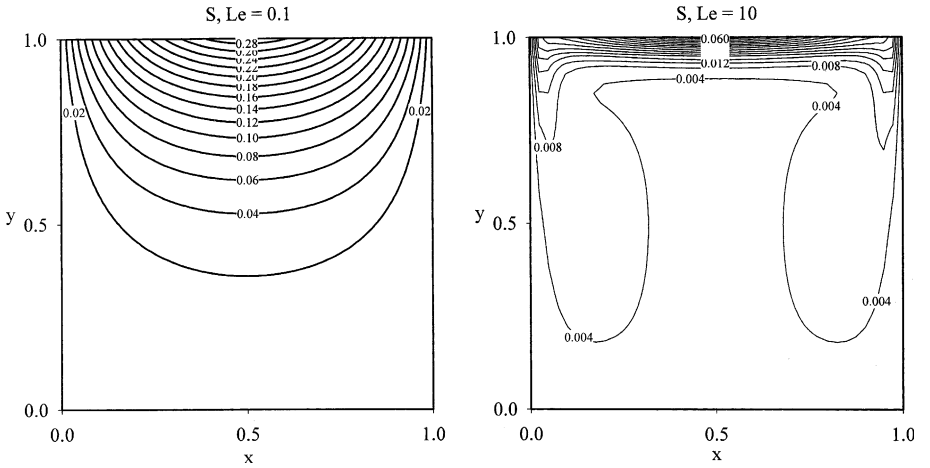

Fig. 7. Concentration at t_f for $Le = 0.1$ and 10, $g_S(x) = \sin(\pi x)$, $Ra = 10^5$.

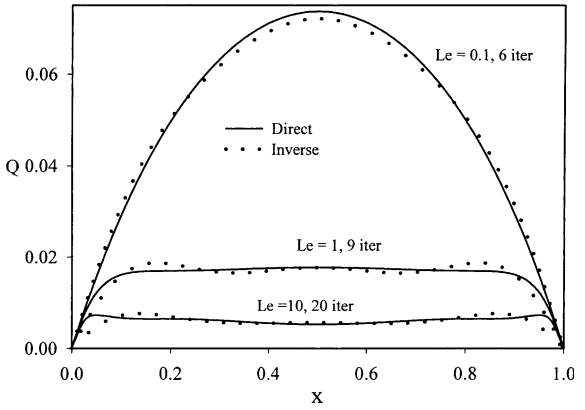

Fig. 8. Predicted heat source profiles at t_f for various Lewis numbers, $g_S(x) = \sin(\pi x)$, $Ra = 10^5$.

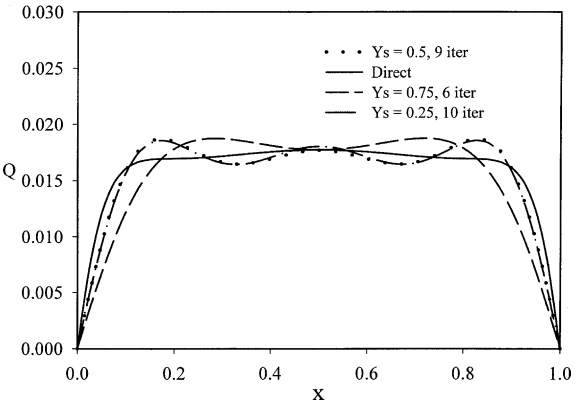

Fig. 9. Predicted heat source profiles at t_f. Influence of sensor position, $g_S(x) = \sin(\pi x)$, $Le = 1$, $Ra = 10^5$.

predicted as accurately by the inverse solution near the vertical walls of the cavity.

The influence of the sensors position is examined in Fig. 9 for $Le = 1$. It is found that convergence is faster for sensors placed at $y = 0.75$ than for sensors placed at $y = 0.50$ or 0.25. But there is otherwise no clear advantage for the accuracy of the solution with the present source model in using one position of the sensors or the other, unlike what is found in the case of an inverse solution for an unknown flux or temperature. For this kind of inverse problem, the most accurate solutions are obtained by moving the sensors closer to the active boundary. In the present case, the solutions obtained from sensors placed at $y = 0.25$ and 0.50 are nearly identical and not qualitatively better or worse than the solution for sensors at $y = 0.75$.

The influence of random noise in the input data can be examined in the convective regime also. Fig. 10 shows the predictions for the evolution with time of the heat source at the middle of the cavity at $x = 0.5$ from noisy input data after 3 and 7 iterations respectively. Comparison of the inverse prediction with the direct solution reveals that the iterative regularisation property of the conjugate method may still be used when convection is present to optimize the inverse solution.

A test case where the concentration gradient $g_S(x)$ imposed at $y = 1$ involves many space Fourier component can be considered. We thus try to recover the heat source resulting from a triangular concentration gradient profile on the top boundary $g_S(x) = 2x$ for $0 < x < 1/2$ and $g_S(x) = 2 - 2x$ for $1/2 < x < 1$. Computations are carried out at $Ra = 10^5$ for a Lewis number $Le = 1$. The evolution in time of the source profile of the direct problem solution depicted in Fig. 11 appears very similar to the inverse solution represented in Fig. 12.

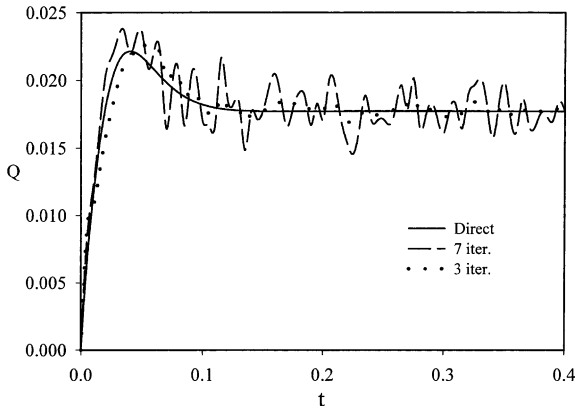

Fig. 10. Heat source prediction versus time at $x = 0.5$, noisy data, $g_S(x) = \sin(\pi x)$, $Le = 1$, $Ra = 10^5$, $\sigma = 0.04$.

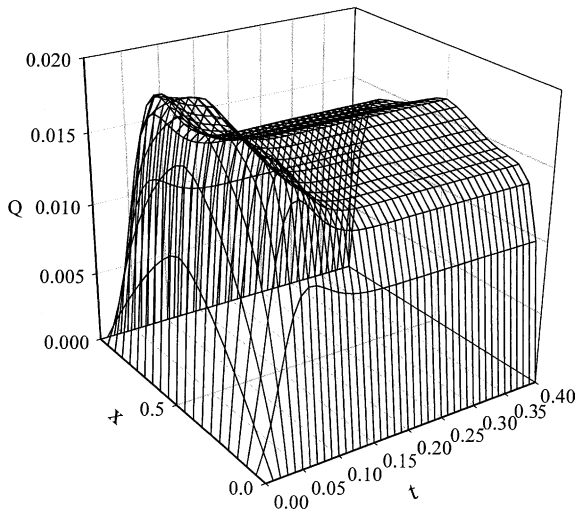

Fig. 11. Heat source Q. Direct solution for triangular concentration flux, $Le = 1$, $Ra = 10^5$.

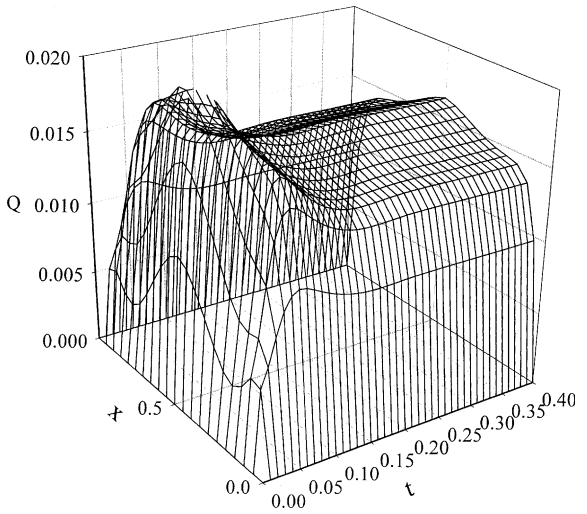

Fig. 12. Heat source Q. Inverse solution, triangular concentration flux, $Le = 1$, $Ra = 10^5$.

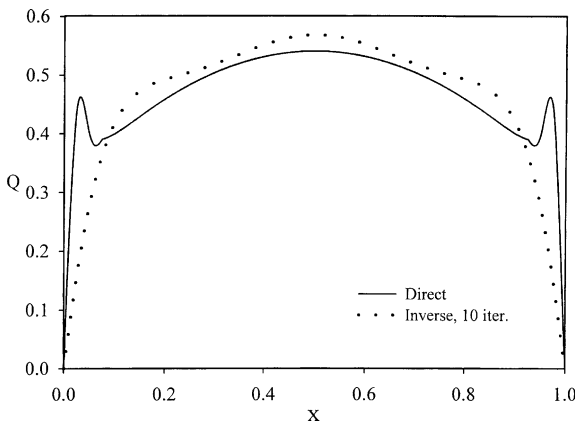

Fig. 13. Predicted heat source profiles at t_f. Non-linear source, $g_S(x) = \sin(\pi x)$, $Le = 1$, $Ra = 10^5$.

For the non-linear source model of Eq. (21), a test was made with the sensors placed at $y = 0.5$, for $g_S = \sin(\pi x)$ and $Le = 1$. The Rayleigh number was also set equal to $Ra = 10^5$ just as for the linear model. It turns out that the values of Q are then larger, but the accuracy of the inverse solution remains qualitatively comparable, at least for this particular model. Fig. 13 shows the steady heat source profiles as a function of x. The inverse solution does not reproduce the rapid, boundary layer-type, variation of the direct solution near the walls, but the overall level of agreement is otherwise satisfactory for an inverse solution when natural convection is involved.

5. Conclusion

A general formulation in two dimensions of the inverse natural convection problem with mass diffusion for an unknown heat source has been presented for the iterative method with adjoint equations and tested for simple source models. Without any a priori information, the method is able to predict over a significant range of Rayleigh numbers an arbitrary volumetric source $Q(x, t)$ which is a function of the solute concentration from temperatures measured by sensors located within the porous matrix. Stable solutions may be obtained from noisy data by stopping the iteration process before the

high frequency components of the random noises start to significantly impair the inverse solution.

Acknowledgements

This research was supported by the Natural Sciences and Engineering Research Council of Canada.

References

[1] K.L. Larsen, D.M. McCartney, Effect of C:N ratio on microbial activity and N retention: bench-scale study using pulp and paper biosolids, Compos. Sci. Utilisation 8 (2000) 147–159.
[2] P.A. Gostomski, J.B. Sisson, R.S. Cherry, Water content dynamics in biofiltration: the role of humidity and microbial heat generation, J. Air Waste Manage. Assoc. 47 (1997) 936–944.
[3] P. Weppen, Process calorimetry on composting of municipal organic wastes, Biomass Bioenergy 21 (2001) 289–299.
[4] A.J. Chamkha, Double-diffusive convection in a porous enclosure with cooperating temperature and concentration gradients and heat generation or absorption effects, Numer. Heat Transfer, Part A 41 (2002) 65–87.
[5] J. Taler, W. Zima, Solution of inverse heat conduction problems using control volume approach, Int. J. Heat Mass Transfer 42 (1999) 1123–1140.
[6] C.Y. Yang, Solving the two-dimensional inverse heat source problem through the linear least-squares error method, Int. J. Heat Mass Transfer 41 (2) (1998) 393–398.
[7] J.V. Beck, Nonlinear estimation applied to the nonlinear inverse heat conduction problem, Int. J. Heat Mass Transfer 13 (1970) 703–716.
[8] J.V. Beck, B. Blackwell, C.R. St-Clair Jr., Inverse Heat Conduction: Ill-posed Problems, Wiley-Interscience, New York, 1985.
[9] A.N. Tikhonov, V.Y. Arsenin, Solutions of Ill-Posed Problems, Winston-Wiley, WA, 1977.
[10] O.M. Alifanov, Inverse Heat Transfer Problems, Springer-Verlag, Berlin Heidelberg, 1994.
[11] A. Moutsoglou, An inverse convection problem, ASME J. Heat Transfer 221 (1989) 37–43.
[12] H.M. Park, O.Y. Chung, An inverse natural convection problem of estimating the strength of a heat source, Int. J. Heat Mass Transfer 42 (1999) 4259–4273.
[13] H.M. Park, W.S. Jung, The Karhunen–Loève Galerkin method for the inverse natural convection problems, Int. J. Heat Mass Transfer 44 (2001) 155–167.
[14] N. Zabaras, G. Yang, A functional optimization formulation and implementation of an inverse natural convection problem, Compt. Meth. Appl. Mech. Eng. 144 (3) (1997) 245–274.
[15] G. Yang, N. Zabaras, An adjoint method for the inverse design of solidification processes with natural convection, Int. J. Numer. Meth. Eng. 42 (6) (1998) 1121–1144.
[16] M. Prud'homme, T.H. Nguyen, Solution of inverse free convection problems by conjugate gradient method: effects of Rayleigh number, Int. J. Heat Mass Transfer 44 (2001) 2011–2027.
[17] R. Fletcher, Practical Methods of Optimization, John Wiley & Sons, New York, 1987.
[18] M. Prud'homme, T.H. Nguyen, Fourier analysis of conjugate gradient method applied to inverse heat conduction problems, Int. J. Heat Mass Transfer 42 (1999) 4447–4460.